International Core Journal of Engineering Volume 9 Issue 12, 2023
ISSN: 2414-1895 DOI: 10.6919/ICJE.202312_9(12).0034

Analysis and Optimization of Dynamic and Static Characteristics of Machining Center Direct-Drive Rotary Table

Jian Wang, Bo Huang*

Sichuan University of Science & Engineering, Yibin 643000, China

Abstract

This paper takes the direct-drive rotary table as the research object, and to reduce its mass and prevent inertia from affecting its machining accuracy, the dynamic and static characterization of the direct-drive rotary table is carried out. The optimization process combines sensitivity analysis, response surface method, and genetic algorithm. A comparison of the data of the prototype and the optimized direct-drive rotary table shows that the optimized parameters not only improve the stiffness and the first-order intrinsic frequency of the direct-drive rotary table but also reduce the mass of the direct-drive rotary table, which can better meet the machining requirements.

Keywords

Rotary Table; Optimized Parameters; Dynamic and Static Characteristics.

1. Introduction

With the continuous development of science and technology, computer technology, and advanced manufacturing technology, higher requirements have been put forward for CNC machine tools, which also bring challenges and opportunities for developing CNC machine tools [1-3]. As one of the core components of the machine tool, the accuracy of its movement and stopping will directly affect the machining accuracy of the parts. The direct-drive rotary table supports and rotates the workpiece, and its dynamic and static characteristics will significantly impact the machining accuracy of the machine tool [4-6].

The current optimization design methods for machine tools are comparative optimization of static characteristics [7], comparative optimization of dynamic characteristics [8], structural topology optimization, and parametric optimal design [9]. Kim et al. [10] used a miniature rotary table as a research object. They used sensitivity analysis for several parameters of this machine tool model, and the optimization results were good.SR Besharati et al. [11] used sensitivity analysis for the structural influence of the gantry structure. The sensitivity analysis was applied to the dimensional parameters with a high degree of influence on the gantry structure, and multi-objective genetic algorithm and hierarchical analysis were applied to optimize the gantry structure. R.Neugebauer et al. [12] applied the knowledge of bionics to optimize the structure of machine tool columns. Shen et al. [13] used the design of a fascia layout based on the growth mechanism of a natural branching system to improve the structure of the machine tool. Liu et al. [14] proposed a bionic design for a CNC rotary table. Liu et al. [14] proposed a bionic optimization design method for a CNC rotary table to improve the mechanical properties of a CNC rotary table under thermal-force coupling. Yi et al. [15] proposed a new method for designing the spindle system considering the spindle and the material efficiency of the machine tool. Liu et al. [16] proposed an optimization method that combines the selection of fascia plate form and layout dimensional optimization and topology optimization. Jiang et al. [17] optimized the whole machine structure using finite element analysis and modal test. A multi-objective genetic algorithm was used for optimization to achieve the light weight of the machining center. Wang et al. [18] workpiece and direct-drive rotary table were studied, and the turntable's maximum

ISSN: 2414-1895 DOI: 10.6919/ICJE.202312_9(12).0034

deformation position and vulnerable parts were analyzed and determined. After multi-objective optimization, the dynamic and static characteristics of the direct-drive rotary table are improved, and the lightweight design is realized.

This paper takes a certain model of a direct-drive rotary table as the research object. It applies the response surface method to the optimization design of a direct-drive rotary table. The dynamic and static analysis of the direct-drive rotary table is carried out, the response surface is constructed using the dimensional parameters of the direct-drive rotary table, and the sensitivity analysis of the design parameters is carried out. The response surface is optimized using a genetic algorithm to obtain the Pareto solution. The results show that the dynamic and static characteristics of the direct-drive rotary table are improved while lightweighting the design.

2. Calculation of Cutting Force

The direct drive rotary table machining methods are divided into turning and milling, respectively. In turn, the C-axis drives the workpiece to rotate as the main motion, and the tool carries out the feeding motion. In milling, the milling cutter is driven by the spindle to rotate rapidly as the central movement, and the C-axis of the rotary table drives the workpiece to rotate at a slower speed with the A-axis swing to process the workpiece. Among the two working modes of the direct-drive rotary table, milling is an example because milling requires higher accuracy than the direct-drive rotary table.

Milling force is a force during the milling process. The force is decomposed in X, Y, and Z directions for easy calculation. The milling force's applied position and the force's decomposition are shown in Fig. 1.

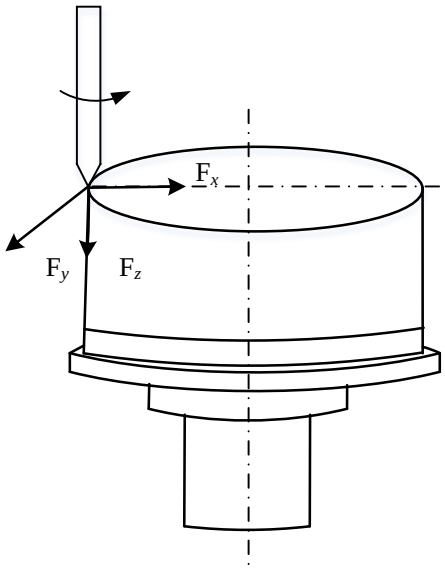

Fig. 1 Direct-drive rotary table milling machining conditions

The milling is done by symmetric end milling, and the following Eq (1) can express its milling force calculation:

$$F_r = 513\alpha_p^{0.9}\alpha_f^{0.74}\alpha_e^{1.0}Zd_0^{-1.0}K_{Fz} \tag{1}$$

Where: αp is the milling depth, αf is the feed per tooth, αe is the milling depth, Z is the number of milling cutter teeth, d0 is the milling diameter, and KFz is the correction factor.

ISSN: 2414-1895 DOI: 10.6919/ICJE.202312_9(12).0034

Table 1. Empirical ratio of each milling force during end milling

Milling conditions	Ratio	Symmetric Milling	Asymmetric Milling	
			Inverse milling	Climb milling
End milling	F_v/F_z	0.85~0.95	0.45~0.70	0.90~1.00
α_e=(0.4~0.8)d_0	F_e/F_z	0.30~0.40	0.60~0.90	0.15~0.30
α_f=(0.1~0.2)mm/z	F_c/F_z	0.50~0.55	0.50~0.55	0.50~0.55

The milling tool is a helical tooth milling cutter with helix angle β=40°~45° and k=0.6~1.2; in this paper, we use a tool with β=42°. k=0.8, the diameter of the cutter is 50mm, and the number of teeth is Z=6.

The milling width is αe=0.6d0=30mm, the milling depth αP can be taken as 2mm by experience, the feed per tooth αf=0.15mm/z, and substituting the parameters into Eq (1) gives Fr=846.55N.

The end milling method adopts symmetric end milling, and the milling force in each direction is:

$$Fx = 0.9Fr = 761.895N,\ Fy = 0.35Fr = 296.29N,\ Fz = -0.52Fr = -440.20N$$

3. Direct-drive Rotary Table Dynamic and Static Characteristics Calculation and Analysis

3.1 Solid Modeling

In the real direct-drive rotary table model in the finite element analysis, when the calculation is huge, many small structures will not have an impact on the overall analysis, so in the establishment of the entity model, the necessary simplification. Simplify the method is mainly: 1. simplify some for the model analysis can be ignored features, such as positioning holes, rounded corners, etc. 2. only analyze the more critical parts of the drive. Use Solidworks to simplify and establish the model in Fig 2.

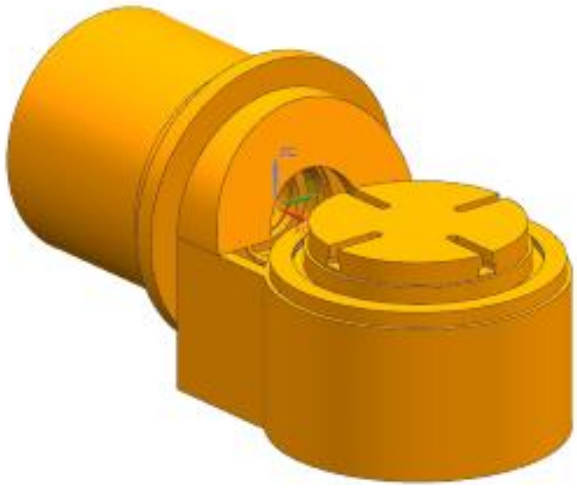

Fig. 2 Three-dimensional model diagram of direct-drive rotary table

3.2 Material Selection

The materials used for the rotary table surface and the workpiece are HT200 and HT250, respectively; 45 steel is used for the mounting sleeve and the rotating spindle, and GCr15 is the material for the YRT bearing. The specific parameters are shown in Table 2:

ISSN: 2414-1895 DOI: 10.6919/ICJE.202312_9(12).0034

Table 2. Material parameters

Material	Density (kg/m^3)	Poisson's ratio	Elastic modulus (Pa)
HT250	7280	0.27	1.2E+11
HT200	7150	0.23	1.13E+11
45 steel	7890	0.30	1.03E+11
GCr15	7810	0.30	2.06E+11

3.3 Mesh Division

The automatic meshing function of Ansys Workbench software was utilized to mesh the direct drive rotary table. 166645 nodes and 67418 meshes were generated, and its resulting mesh diagram is shown in Fig. 3:

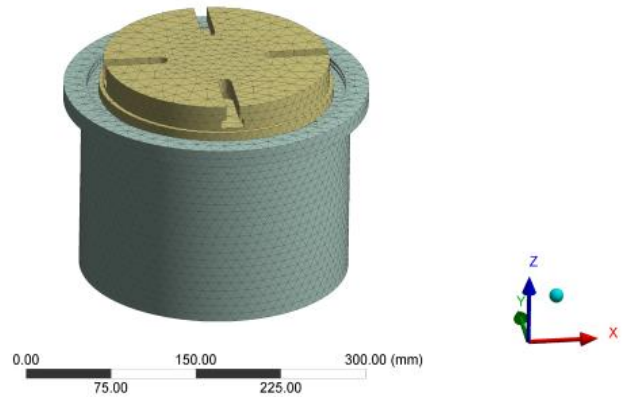

Fig. 3 Finite element model of direct-drive rotary table

3.4 Static Characterization

Fixed constraints are added at the rotary table bearings of the C-axis of the direct-drive rotary table, and the milling force is added at the maximum radius of the top of the workpiece. The workpiece and rotary table deformation and stress are at their maximum values. The deformation is shown in Fig. 4:

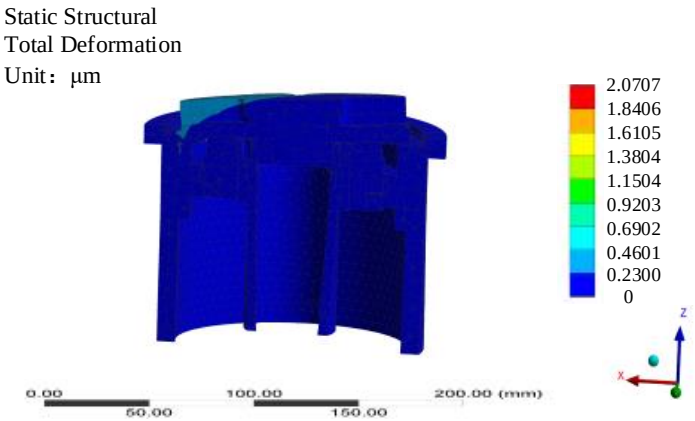

Fig. 4 Deformation nephogram under milling condition

The analysis of the deformation nephogram shows that under the milling condition, the maximum value of deformation occurs at the position of contact between the workpiece and the tool, which is about 2μm. The deformation of the direct-drive rotary table is smaller. The maximum value is at the position of the edge of the rotary table surface, and its deformation is about 0.36μm.

ISSN: 2414-1895 DOI: 10.6919/ICJE.202312_9(12).0034

3.5 Structural Dynamic Characterization

The modal analysis gives the object's intrinsic frequency and mode of vibration. The intrinsic frequency is an inherent characteristic of the object, so there is no need to apply external loads. The first six order modes are obtained after modal analysis, as shown in Fig. 5. The first-order intrinsic frequency of the object is most likely to form resonance during processing, so the focus is on the first-order modes.

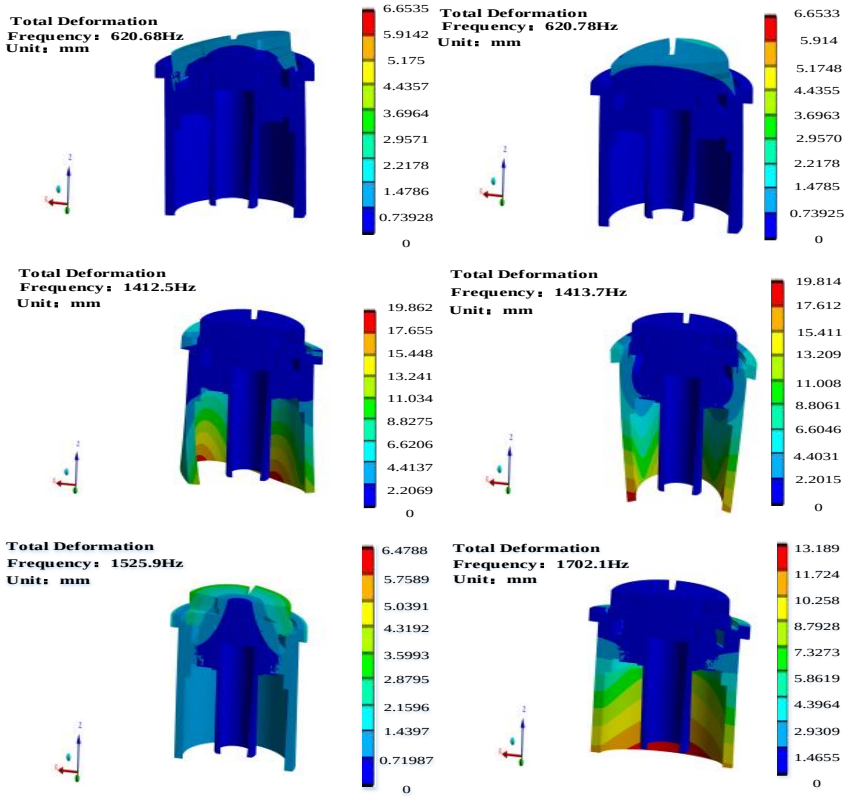

Fig. 5 The first six order modes of direct-drive rotary table

Table 3. The first six vibration modes and natural frequencies of direct drive turntable under milling condition

Order	Frequency (Hz)	Vibration mode
1	620.68	Rotary table surface and mounting sleeve oscillate along the x-axis
2	620.78	Rotary table surface and mounting sleeve oscillate along the y-axis
3	1412.5	Mounting sleeve oscillates in the x-axis direction
4	1413.7	Mounting sleeve oscillates in the y-axis direction
5	1525.9	Rotary table surface and mounting sleeve rotate around the z-axis.
6	1702.1	Rotary table surface and mounting sleeve rotate around the y-axis.

Comparison with the C-axis operating parameters of the direct-drive rotary table shows that the first-order modal of the direct-drive rotary table meets the requirements, and it should be ensured that its first-order modal value does not decrease during the optimization.

ISSN: 2414-1895 DOI: 10.6919/ICJE.202312_9(12).0034

4. Dynamic and Static Multi-objective Optimization Design of Direct-drive Rotary Table

The data of the prototype direct-drive rotary table: the mass of the C-axis is 100.93 kg, the maximum deformation under milling conditions is 0.002059 mm, and the first-order intrinsic frequency is 620.68 Hz. To realize the lightweight design and, at the same time, to improve the machining accuracy, the direct-drive rotary table is designed to be optimized. The optimization objectives are table mass, first-order modal, and stiffness, and the constraints are not to reduce the stiffness and first-order intrinsic frequency. The constraint range set is ±10% of each optimization parameter. The optimization parameters are determined based on the direct drive rotary table structure. Solidworks software was used to parameterize the design of these selected parameters.

4.1 Direct-drive Rotary Table Response Surface Design Methodology

Six optimization parameters are selected as shown in Fig. 6:

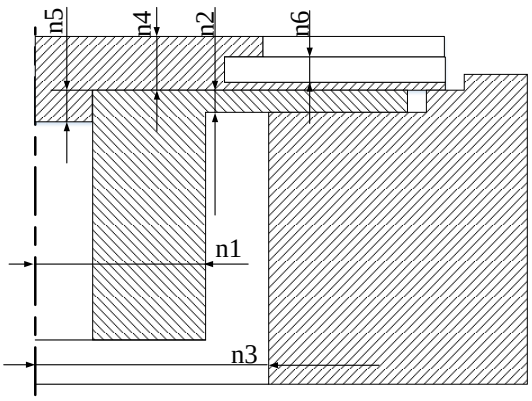

Fig. 6 Design parameters of direct-drive rotary table

We take these six dimensions as the optimization parameters, take the maximum deformation as ωmax, the mass as m, and the first-order intrinsic frequency as f as the optimization objectives, and establish the following optimization model:

$$\begin{cases} Find: X = [x1, x2, x3, x4, x5, x6] \\ min: \ F(X) = min(m, f, \omega_{max}) \\ s.t. \quad m - 100.93 \leq 0 \\ \quad\quad \omega_{max} - 0.002059 \leq 0 \\ \quad\quad f - 620.68 \geq 0 \end{cases} \tag{2}$$

Where: X is the vector of design variables; F(X) is the objective function; xi is each design variable; m is the total mass of the direct-drive rotary table, kg; f is the first-order modal state of the direct-drive rotary table under milling condition, Hz; and ωmax is the maximum deformation of the direct-drive rotary table under milling condition, mm.

The Center Composite Design of Experiments (CCD) is used to determine the experimental points in this experiment. The accuracy can be guaranteed, and the number of design points is less. The points are designed using CCD, and the values corresponding to the design points are calculated, through which the response surface model is built.

ISSN: 2414-1895 DOI: 10.6919/ICJE.202312_9(12).0034

The response surface method is a global approximation method similar to Lagrange expansion, and the mathematical principle of using it to solve the response surface method is represented by the following Eq (3):

$$y(X)=\beta_0+\sum_{i=1}^{n}\beta_i x_i^2+\sum_{i=1}^{n}\beta_{ii}x_i^2+\sum_{i=2}^{n}\sum_{j=1}^{i-1}\beta_{ij}x_i x_j \tag{3}$$

Where: X represents the set of all design points X=(x1, x2, …, xn), β is the number of design points determined by the CCD, and L is the minimum number of design points, L=(n+1)(n+2)/2. when using the least squares method to determine β, where L is the minimum number of design points determined by the CCD method. The number of design points must be greater than L.

The design point consists of three parts: (1) One or more center points determine the error accuracy and estimation. (2) 2n axial points, which are taken to different values from 1 to $\sqrt{n}$ in other CCD methods, and the axial points represent quadratic terms on the response surface, each of which is a two-pole value. (3) $2^{n-\delta}$ analytical factorization points. Their positions on the diagonal are used to estimate the first-order terms.

Through the optimization function of finite element software, 46 design points were obtained, the response surface was constructed through the calculation of the design points, and the statistical data of the normalization method was used to obtain the influence degree of the change of the optimization parameter n1-n6 on the optimization target in a more intuitive way. The influence of the obtained response surface on the stiffness, frequency, and mass is shown in Fig. 7:

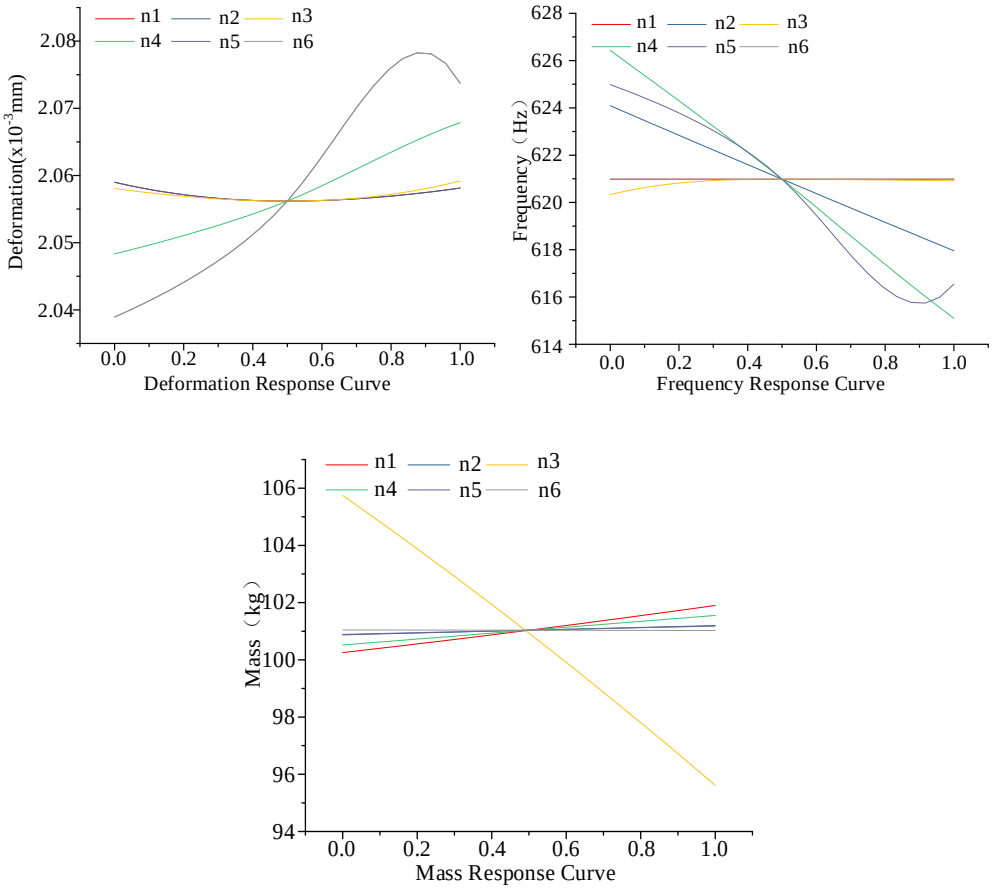

Fig. 7 Response curve of each target

ISSN: 2414-1895 DOI: 10.6919/ICJE.202312_9(12).0034

It can be seen that the design point is related to the 1st-order intrinsic frequency, stiffness, and mass of the rotary table, but the correlation is irregularly distributed. Therefore, it is impossible to increase or decrease individual parameters to improve the dynamic and static characteristics of the direct-drive rotary table and reduce its mass. It is challenging to optimize the parameters simultaneously, and multi-objective optimization is required to obtain the optimum values.

4.2 Sensitivity Analysis of Rotary Table

To improve the efficiency of the optimization, a sensitivity analysis of the six parameters of the direct-drive rotary table is carried out to determine the parameters that have a greater influence on the rotary table mass, frequency, and stiffness. The theoretical basis of sensitivity can be expressed by Eq (4):

$$S = \frac{df(x)}{dx} \tag{4}$$

Where: f(x) is the derivable function, and S is the sensitivity.

Calculating the sensitivity of the six parameters to the mass, stiffness, and frequency of the rotary table yields the results shown in Fig. 8~ Fig. 10:

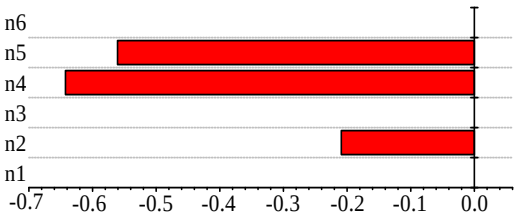

Fig. 8 Frequency sensitivity correlation

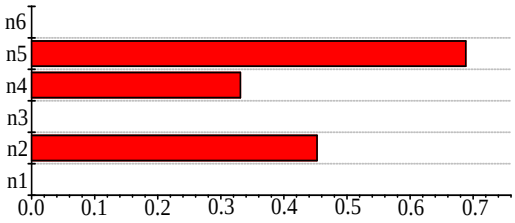

Fig. 9 Deformation sensitivity correlation

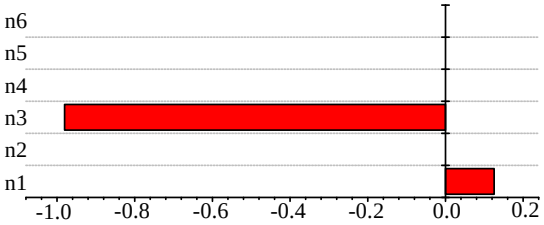

Fig.10 Total mass sensitivity correlation

From Fig. 8-Fig. 10, it can be seen that: the parameters sensitive to frequency are n2, n4, and n5, and all are negatively correlated; the parameters sensitive to deformation are also n2, n4, and n5, and all are positively correlated; and the parameters sensitive to the total mass are n1 and n3, of which n1 is negatively correlated and n3 is positively correlated.

4.3 Optimization Results

Focus on five parameters: n1, n2, n3, n4 and n5. Using the response surface optimization design module of the finite element software, minimizing the mass of the rotary table, maximizing the 1st order intrinsic frequency, and minimizing the deformation are taken as the objectives, and the optimal solutions of three groups of Parato are obtained using the multi-objective genetic algorithm.

Since it is difficult to simultaneously reach the optimum between the objectives during the optimization process, multi-objective optimization often produces a series of Pareto solutions. Regarding the objective function, it is impossible to compare the advantages and disadvantages of these solutions. Solving a multi-objective optimization problem is to find as many representative Pareto optimal solutions as possible without preference. After calculating the uniformly distributed

ISSN: 2414-1895 DOI: 10.6919/ICJE.202312_9(12).0034

Pareto optimal solutions, the optimal optimization results are selected objectively according to the design requirements and actual engineering experience. NSGA-II is considered one of the most effective multi-objective genetic algorithms, which can reduce the scale of the computation and preserve the diversity of the effective elites and populations. The changes in the optimized size parameters and the objective function selected before and after the optimization are shown in Table 4 and Table 5.

Table 4. Original and optimized dimensional parameters (Unit: mm)

Design point	Original data	Optimized data 1	Optimized data 2	Optimized data 3
n1	82.14	73.92	88.57	81.38
n2	13.16	11.84	12.29	13.37
n3	205.78	226.35	225.55	234.28
n4	22.81	20.53	20.61	19.24
n5	10.53	9.48	9.64	7.29
n6	7.27	7.90	6.69	10.83

Table 5. Optimal values and original values

	Mass/kg	Frequency/Hz	Deformation/μm
Optimal value 1	94.00	634.85	2.02
Optimal value 2	95.18	631.35	2.02
Optimal value 3	95.78	632.60	2.02
Original values	100.93	620.68	2.06

Since the mass has the largest weight in the optimization, the optimized value 1 is chosen as the optimal solution. After optimization, the mass of the direct-drive rotary table is reduced by 6.87%, the first-order intrinsic frequency is increased by 2.28%, and the deformation is reduced by 1.99% under the same load. The optimization objectives are all optimized over the initial values, and the purpose of optimization is achieved.

5. Conclusion

The structure of the direct-drive rotary table is analyzed, and the milling model of the direct-drive rotary table is established with milling as the research working condition. Calculate the milling force and the three components of the force, simulation, and analysis in the finite element software to obtain the dynamic and static characteristics of the direct-drive rotary table. To ensure that the dynamic and static characteristics of the direct-drive rotary table meet the machining requirements while realizing the lightweight design of the direct-drive rotary table, multi-objective optimization is carried out for the direct-drive rotary table. Six dimensions of the direct-drive rotary table are selected as optimization parameters. The direct-drive rotary table's first-order intrinsic frequency, mass, and stiffness are taken as the objective functions. The direct-drive rotary table is optimized in the optimization module of the finite element software. The results show that the optimized direct-drive rotary table has better dynamic and static characteristics and reduces the mass by 6.87%, which can be better adapted to the machining requirements.

ISSN: 2414-1895 DOI: 10.6919/ICJE.202312_9(12).0034

Acknowledgments

The authors gratefully acknowledge the financial support from The Innovation Fund of Postgraduate, Sichuan University of Science & Engineering(grant number Y2022047).

References

[1] Pedrammehr, S.; Mahboubkhah, M.; Khani, N. A study on vibration of Stewart platform-based machine tool table. Int. J. Adv. Manuf. Technol. 2013, 65, 991–1007.

[2] Liu, Z.; Zhan, C.; Zhao, Y.; Li, X.; Xia, L.; Cai, L. Modeling and analysis of the dynamic behaviors of a quantitative type hydrostatic rotary table. J. Mech. Eng. 2015, 51, 75–83.

[3] Li, T.; Wu, C.; Shen, L.; Kong, X.; Ding, X. Improving machine tool dynamic performance using modal prediction and sensitivity analysis method. J. Mech. Eng. 2019, 55, 178–186.

[4] Chen, J.; Lin, S.; He, B. Geometric error measurement and identification for rotary table of multi-axis machine tool using double ballbar. Int. J. Mach. Tools Manuf. 2014, 77, 55.

[5] Ding, W.; Zhu, X.; Huang, X. Effect of servo and geometric errors of tilting-rotary tables on volumetric errors in five-axis machine tools. Int. J. Mach. Tools Manuf. 2016, 104, 44.

[6] Alessandro, V.; Gianni, C.; Antonio, S. Axis geometrical errors analysis through a performance test to evaluate kinematic error in a five axis tilting-rotary table machine tool. Precis. Eng. 2015, 39, 224–233.

[7] Kang, Y.; Chang, P.; Tsai, W.; Chen, C. Integrated “CAE” strategies for the design of machine tool spindle-bearing systems. Finite Elem. Anal. Des. 2001, 37, 485–511.

[8] Huo, D.; Cheng, K.; Wardle, F. A holistic integrated dynamic design and modelling approach applied to the development of ultraprecision micro-milling machines. Int. J. Mach. Tools Manuf. 2010, 50, 335–343.

[9] Altintas, Y.; Brecher, C.; Weck, M.; Witt, S. Virtual machine tool. CIRP Annals 2005, 54, 651–674.

[10] Kim, D.; Jung, S.; Lee, J.; Chang, S. Parametric study on design of composite-foam-resin concrete sandwich structures for precision machine tool structures. Compos. Struct. 2006, 75, 408–414.

[11] Besharati, S.; Dabbagh, V.; Amini, H.; Sarhan, A.; Akbari, J. Multi-objective selection and structural optimization of the gantry in a gantry machine tool for improving static, dynamic, and weight and cost performance. Concurr. Eng. Res. Appl .2016, 24, 83–93.

[12] Neugebauer, R.; Wabner, M.; Ihlenfeldt, S.; Friess, U.; Schneider, F. Bionics Based Energy Efficient Machine Tool Design. Procedia CIRP 2012, 3, 561–566.

[13] Shen, L.; Ding, X.; Li, T.; Kong, X.; Dong, X. Structural dynamic design optimization and experimental verification of a machine tool. Int. J. Adv. Manuf. Technol. 2019, 104, 3773–3786.

[14] Liu, S.; Lin, M. Bionic optimization design for a CNC turntable based on thermal-mechanical coupling effect. J. Braz. Soc. Mech. Sci. 2020, 42, 253.

[15] Yi, Q.; Li, C.; Ji, Q.; Zhu, D.; Jin, Y. Design optimization of lathe spindle system for optimum energy efficiency. J. Cleaner Prod. 2020, 250, 119536.

[16] Meng, D.; Yang, S.; He, C.; Wang, H.; Lv, Z.; Guo, Y.; Nie, P. Multidisciplinary design optimization of engineering systems under uncertainty: A review. Nt. J. Struct. Integr. 2022, 13, 565–593.

[17] Liu, C.; Tan, F.; Wang, L.; Cai, Z. Research on optimization of column structure design for dynamic performance of machine tool. J. Mech. Eng. 2016, 52, 161–168.

[18] Huang, B; Wang, J; Tan, B. Analysis and Optimization of Dynamic and Static Characteristics of Machining Center Direct-Drive Turntable. Appl. Sci.2022,12(19).